Selective Oxidation of Pharmaceuticals and Suppression of Perchlorate Formation during Electrolysis of Fresh Human Urine

James A. Clark,[†] Yuhang Yang,[‡] Nathanael C. Ramos,[†] Michael C. Dodd,[§] and Hugh W. Hillhouse[†,]*

† Department of Chemical Engineering, Clean Energy Institute, Molecular Engineering & Sciences Institute, University of Washington, Seattle, Washington 98195-1750

‡ Department of Materials Science and Engineering, University of Washington, Seattle, Washington 98195-2120

§ Department of Civil & Environmental Engineering, University of Washington, Seattle, Washington 98195-2700

* Email: h2@uw.edu

Abstract

Many pharmaceutical compounds are excreted unchanged or as active metabolites via urine. They pass through conventional wastewater treatment processes, and present a risk to aquatic ecosystems and humans. Point-source remediation of source-separated urine provides a promising alternative to destroy pharmaceuticals before dilution with wastewater. Electrochemical advanced oxidation processes are one possible option for degrading pharmaceuticals in urine, but they often lead to the formation of oxidation byproducts (OBPs) including chlorate, perchlorate, and halogenated organics at hazardous concentrations due to high background chloride concentrations. Here, we show that the high urea content of fresh human urine suppresses the formation of oxychlorides by inhibiting formation of $HOCl/OCl^-$ during electrolysis, while still enabling the oxidation of pharmaceuticals by $^{\bullet}OH$ due to the slow rate of urea oxidation by $^{\bullet}OH$. This results in improved performance when compared to equivalent treatment of hydrolyzed aged urine. This (primarily indirect) electrochemical oxidation scheme is shown to degrade the model pharmaceuticals cyclophosphamide and sulfamethoxazole with surface-area-to-volume-normalized pseudo-first-order observed rate constants greater than 0.08 cm/min in authentic fresh human urine matrixes. It results in two orders-of-magnitude decrease in pharmaceutical concentrations in 2 hours while generating three orders-of-magnitude lower oxychloride byproduct concentrations in synthetic fresh urine as compared to synthetic hydrolyzed aged urine matrixes. Importantly, this proof-of-principle shows that simple and safe electrochemical methods can be used for point-source-remediation of pharmaceuticals in fresh human urine (before storage and hydrolysis), without formation of significant oxychloride byproducts.

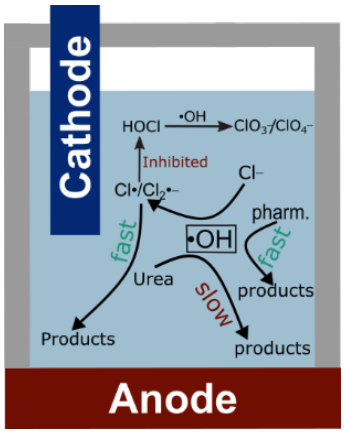

TOC Figure. (no caption)

1. Introduction

Many pharmaceutical compounds are not sufficiently deactivated during typical wastewater treatment and eventually end up being discharged into the environment. These pharmaceuticals may threaten aquatic ecosystems,[1] contribute to the development of antibiotic-resistant bacteria,[2] and can eventually return to human drinking water supplies.[3] Chemical oxidation and advanced oxidation processes (AOPs) are an important means of addressing this growing problem because of their ability to degrade organic contaminants via oxidizing species (i.e., $^{\bullet}OH$, O_3 , etc., in addition to HOCl, $Cl^{\bullet}$, and $Cl_2^{\bullet-}$ in free chlorine or chloride containing solutions) through chemical, photochemical, or electrochemical means.[4-6] Numerous studies have examined pharmaceutical degradation using AOPs,[7-13] and there are many proposed strategies ranging from large-scale implementation as a tertiary treatment step at centralized wastewater treatment facilities (WWTFs) to small-scale decentralized implementation to treat point sources.

Point-source treatment for pharmaceutical pollutants at homes, businesses, and hospitals is attractive because the compounds may be treated before they are diluted by a factor of 1,000 with other wastewater. However, strategies that employ the addition of chemical agents[14] (Fenton's

reagent, peroxides or other oxidants or catalysts) are unsuitable for distributed or in-home use due to safety concerns regarding the handling of oxidants, removal or disposal of wastes from the process, and high-cost. This study focuses on the underlying chemistry relevant to application of electrochemical advanced oxidation processes (EAOPs) for treatment of fresh urine. These EAOPs have the potential to enable point-source approaches to treatment of fresh urine that are safe and easy to operate since they do not require the addition of oxidants or generate new waste streams. The two biggest challenges facing this approach are the relatively low concentrations of pharmaceuticals and the potential formation of oxidation byproducts (OBPs) that can result from oxidation of co-occurring chloride and other halides. Many studies highlight that OBPs formed during AOPs can create serious environmental and human health problems on their own,[15] including chlorate, perchlorate, haloacetic acids, aliphatic halide species, haloacetonitriles, haloacetamides, and nitrosamines. The halogenated OBPs are mostly chlorinated species; however, brominated and iodinated species may be present at much lower concentrations but with higher toxicity.[16] Thus, there is a need to develop novel EAOPs or improved approaches to employing existing EAOPs that enable high efficiency toward pharmaceutical destruction while preventing or mitigating OBP formation.

The dominant route for the elimination of non-volatile pharmaceutical excretion is via urine.[17-19] Of the top 200 prescribed drugs in the U.S., roughly 30% of the ingested pharmaceutical load is excreted unchanged via urine, while ~65% is metabolized and excreted via both urine and feces with the remaining ~5% via biliary elimination.[20] Further, some metabolites retain key pharmacological properties of parent compounds, and many of them will remain active.[21] Thus, targeting treatment of urine (before dilution) is an attractive strategy to reduce pharmaceutical pollution. While the high electrical conductivity of urine (due primarily to chloride salts) is an

advantage for EAOPs, the presence of high concentrations of urea or ammonium (over two orders of magnitude greater than pharmaceutical concentrations) could be a major hurdle forcing one to oxidize most of the urea before significant oxidation of the pharmaceuticals. In this study, we show that the unusually slow rate of urea oxidation by the hydroxyl radical (•OH) (7.9×10^5 $M^{-1}s^{-1}$ for urea[22] vs. 2×10^9 $M^{-1}s^{-1}$ for cyclophosphamide[23] and 6.2×10^9 $M^{-1}s^{-1}$ for sulfamethoxazole[24]) provides a de facto selectivity for •OH attack on the other organics (**Scheme 1**, r_1 and r_3).

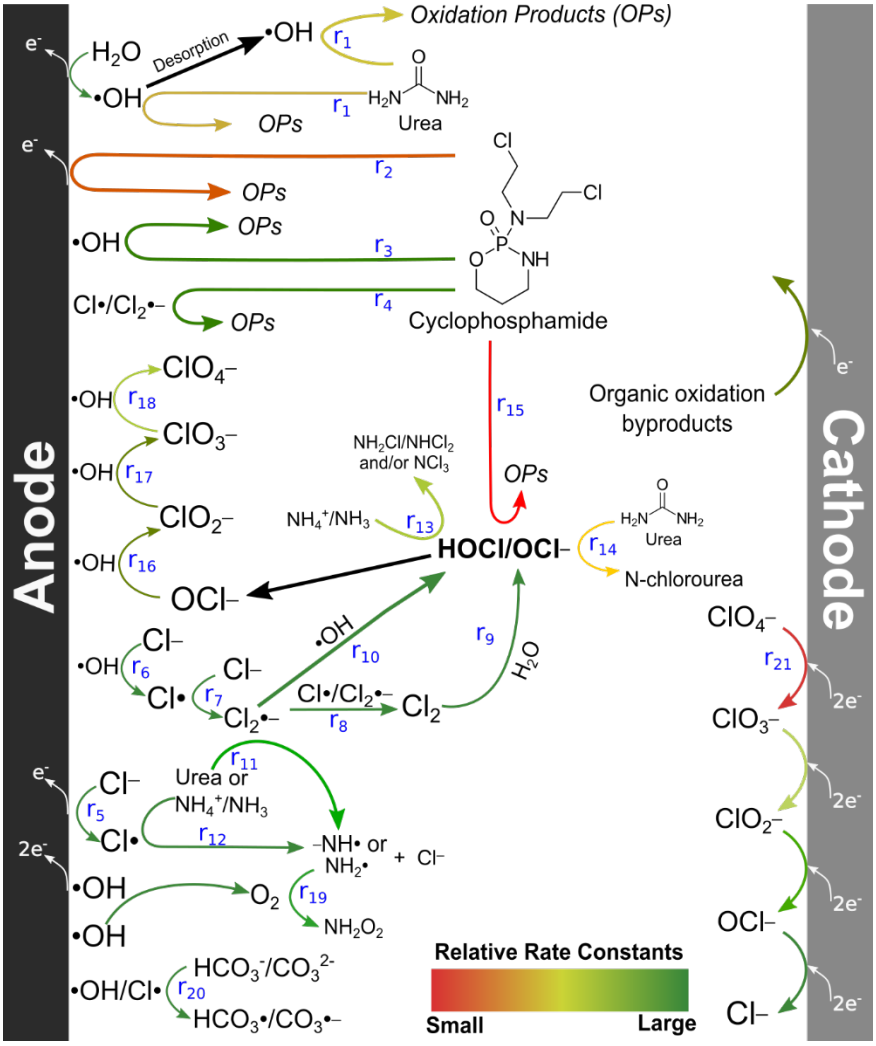

Scheme 1. Relative rate constants for important reactions during the electrolysis of pharmaceuticals in urine matrixes (with cyclophosphamide as an example pharmaceutical in an undivided cell setup). The formation of chlorate (ClO_3^-) and perchlorate (ClO_4^-) can be supressed by the presence of high nitrogen concentration (i.e., urea or NH_4^+/NH_3). Divided cell architectures will block r_{21} and subsequent reactions. The relative rates of these reactions are important to

consider to successfully decrease pharmaceutical concentrations while not generating OBPs. The color coding indicates the relative range of large to small rate constants. It is noteworthy that reactions $r_{11\text{-}14}$ involving urea and NH_4^+/NH_3 as reactants with high concentration will have high reaction rates, even though the second-order rate constants for these reactions are lower relative to other depicted reactions. The black arrows represent the transport of species. Furthermore, $^{\bullet}OH$, $Cl^{\bullet}$ and $Cl_2^{\bullet-}$ depicted at the anode surface may also desorb and diffuse outward through a relatively stagnant near-anode region. Likewise, Cl^-, urea, and the pharmaceuticals diffuse from bulk solution toward the anode as they are consumed at the anode or in the near-anode stagnant region. See Section 3.3 for discussion of the importance of mass transport in galvanostatic experiments.

Several studies have examined the application of EAOPs to various urine matrixes and have shown differences in the generation of OBPs. Studies have examined electrochemical treatment of synthetic urine[25-31] and human-generated stored urine,[16, 32-35] for multiple purposes including pharmaceutical degradation, distributed wastewater treatment, and nutrient recovery (for nitrogen and phosphorus). Interestingly, the concentrations of the OBPs reported for roughly equivalent oxidation treatments are vastly different. For example, many studies report large amounts (>10 mM) of generated ClO_4^- after 30 A·hr/L of treatment using a boron-doped diamond (BDD) electrode,[16, 29, 30, 35] while a similar report measured ClO_4^- below the detection limit for the same normalized charge passed.[31] One critical difference between these studies that may explain these differences is the composition of the matrix. Fresh urine (authentic and synthetic) has a high concentration of urea – averaging 15 g/L (250 mM),[36] and a pH of about 6. By contrast, stored hydrolyzed authentic urine has a urea concentration of ~0 mM, ammonium concentration of 30-120 mM, bicarbonate/carbonate concentration of 25-30 mM, and a pH of about 9.[32] This is due to naturally abundant bacterial urease which hydrolyzes urea to form ammonium, bicarbonate, and hydroxide (eq 1).

$$(NH_2)_2CO + 3H_2O \xrightarrow{\text{urease}} 2NH_4^+ + HCO_3^- + OH^- \quad (1)$$

This reaction happens rapidly, with one study finding that urea is nearly completely hydrolyzed within 5 hours of storage in a pipe.[37] The concentration of ammonium decreases over time with

elevation of pH and volatilization of ammonia if the solution is open to the atmosphere. The concentrations of carbonate species also decrease due to precipitation as $CaCO_3$. [38, 39]

The hydrolysis of urea to NH_4^+ and HCO_3^-, along with the volatilization of NH_3 and precipitation of CO_3^{2-}, can have major impacts on the oxidation pathways during the application of an EAOP. One of the strongest oxidants produced in an EAOP is $^{\bullet}OH$ ($E^{0'}$ ($^{\bullet}OH$, H^+/H_2O) = 2.32 V at pH 7),[40] which reacts rapidly with most organic molecules by either addition or hydrogen abstraction (**Scheme 1**, r_3), with second-order rate constants typically in the range of $10^9 \sim 10^{10}$ $M^{-1}s^{-1}$.[22] However, this important radical is scavenged by NH_3 and HCO_3^-/CO_3^{2-} in hydrolyzed urine much faster than by the urea in fresh urine (eqs. 2-5), with respective pseudo-first-order scavenging rate constants, k' = 2.6 × 10^7 s^{-1} and 2.0 × 10^5 s^{-1} (**Text S1**):[22, 41]

urea + $^{\bullet}OH \rightarrow$ products $\quad k_2 = 7.9 \times 10^5\ M^{-1}s^{-1}$ (2)

$NH_3 + {}^{\bullet}OH \rightarrow {}^{\bullet}NH_2 + H_2O \quad k_3 = 9.0\times10^7\ M^{-1}s^{-1}$ (3)

$HCO_3^- + {}^{\bullet}OH \rightarrow CO_3^{\bullet-} + H_2O \quad k_4 = 8.5\times10^6\ M^{-1}s^{-1}$ (4)

$CO_3^{2-} + {}^{\bullet}OH \rightarrow CO_3^{\bullet-} + OH^- \quad k_5 = 3.9\times10^8\ M^{-1}s^{-1}$ (5)

While the amino radical (E^0 ($^{\bullet}NH_2/NH_3$) = 0.6 V)[42] and carbonate radical ($E^{0'}$ ($CO_3^{\bullet-}$/ CO_3^{2-}) = 1.57 V)[40], resulting from reactions of $^{\bullet}OH$ with NH_3 and HCO_3^-/CO_3^{2-}, may also provide some oxidizing power, their second-order rate constants with most organic molecules are more than 3 orders of magnitude smaller than $^{\bullet}OH$.[42-45] Further, $^{\bullet}NH_2$ will be rapidly scavenged by dissolved O_2 (**Scheme 1**, r_{19}).[41] In urine matrixes with high chloride concentrations (~100 mM), reaction of $^{\bullet}OH$ with Cl^- (**Scheme 1**, r_6) and direct anodic electron transfer from Cl^- (**Scheme 1**, r_5) will also lead to formation of the chlorine radicals, $Cl^{\bullet}$ (E^0 ($Cl^{\bullet}/Cl^-$) = 2.43 V)[40] and $Cl_2^{\bullet-}$ (E^0 ($Cl_2^{\bullet-}/Cl^-$) = 2.13 V)[40]. They may also contribute to degradation of organic molecules (**Scheme 1**, r_4), with rate constants for $Cl^{\bullet}$ typically spanning a similar range as for $^{\bullet}OH$, and rate constants for $Cl_2^{\bullet-}$ typically

1-2 orders of magnitude lower than for $^{\bullet}OH$.[22, 42, 46] The rate constants do not appear to have been reported for reactions of $Cl^{\bullet}$ or $Cl_2^{\bullet-}$ with urea or NH_4^+/NH_3. However, observations from previous work suggest that these radicals likely react rapidly with both nitrogen species. Therefore, both urea and NH_4^+/NH_3 likely serve as scavengers of $Cl^{\bullet}$ and/or $Cl_2^{\bullet-}$. (**Scheme 1**, r_{11} and r_{12}).[27, 47-50]

In addition to their effects on organic contaminant degradation, the concentration of urea or NH_4^+/NH_3 may affect the sequence of chloride oxidation to free chlorine (FC – primarily HOCl and OCl^-, and to a lesser extent Cl_2 and/or Cl_2O) and higher oxidation states (eg. ClO_3^- and ClO_4^-). In fresh and hydrolyzed urine, FC is formed via radical-driven or direct anodic oxidation of Cl^- (**Scheme 1**, $r_{5\text{-}10}$).[51] As noted above, urea or NH_4^+/NH_3 appear likely to serve as effective scavengers of $Cl^{\bullet}$ and/or $Cl_2^{\bullet-}$ in either fresh or hydrolyzed urine. This could contribute to suppression of FC formation by hindering recombination and/or disproportionation reactions involving $Cl^{\bullet}$ and $Cl_2^{\bullet-}$ (several of which lead to direct formation of Cl_2)[52]. In hydrolyzed urine with a pH of 9, NH_4^+/NH_3 ($k_{HOCl,NH3} = 3.1 \times 10^6$ $M^{-1}s^{-1}$ $M^{-1}s^{-1}$)[53] should react with FC with an apparent second-order rate constant of ~3×10^4 $M^{-1}s^{-1}$ (not corrected for ionic strength) (**Scheme 1**, r_{13}). It results in an anticipated maximal pseudo-first-order FC scavenging rate constant of ~2×10^4 s^{-1} (and $t_{1/2} \sim 4 \times 10^{-5}$ s) at the 500 mM NH_4^+/NH_3 level of freshly hydrolyzed urine (with diminishing rate constant values as NH_3 volatilizes from the urine during storage). In fresh urine with a pH of 6, urea ($k_{HOCl,urea} = 0.63$ $M^{-1}s^{-1}$)[54] should react with FC with an apparent second-order rate constant of ~0.6 $M^{-1}s^{-1}$ (**Scheme 1**, r_{14}). This leads to a lower, but still high pseudo-first-order FC scavenging rate constant of ~0.2 s^{-1} (and $t_{1/2} \sim 4$ s). In either case, the presence of high levels of NH_4^+/NH_3 or urea should contribute to suppression of the further oxidation of HOCl/OCl^- into ClO_3^- and ClO_4^- (**Scheme 1**, $r_{16\text{-}18}$).

Many reports highlight large amounts of OBPs generated from EAOPs applied to urine. While electrochemical remediation of various OBPs has been demonstrated, including alkyl halides,[55, 56] haloacetic acids,[57] nitrosamines,[58] ClO_3^-,[59] and ClO_4^-,[60-62] preventing them from forming is a preferred approach. ClO_4^- is the most challenging to remediate due to its high stability among all the OBPs generated during electrolysis of urine. ClO_4^- has a large electrochemical activation barrier for reduction to ClO_3^- of 120 kJ/mole,[63] which makes its reduction very sluggish (**Scheme 1**, r_{21}). The slow kinetics of ClO_4^- reduction accentuate the need that EAOPs not generate significant quantities of ClO_4^-, even if an OBP remediation step is applied after oxidation.

In this work, we show the advantages of conducting electrochemical oxidation of pharmaceuticals in fresh urine (at point of generation) as opposed to hydrolyzed (without loss of NH_3) or hydrolyzed aged urine (with loss of NH_3). We demonstrate that urea (and/or NH_4^+/NH_3) effectively inhibits the oxidation pathway toward ClO_4^-, likely due to scavenging of $Cl^\bullet$ and/or $Cl_2^{\bullet-}$ (**Scheme 1**, r_{11} and r_{12}) or rapid sequestration of HOCl (**Scheme 1**, r_{13} and r_{14}). Meanwhile, the urea in fresh urine inhibits the oxidation of pharmaceuticals much less than the NH_4^+/NH_3 and HCO_3^-/CO_3^{2-} in hydrolyzed urine due to urea's lower reactivity toward $^\bullet OH$ (**Scheme 1**, $r_{1,}$ r_3 and r_{20}). Accordingly, the electrochemical oxidation rates of the pharmaceuticals investigated are higher in synthetic fresh urine matrixes than in synthetic hydrolyzed and hydrolyzed aged urine matrixes. Thus, this work provides a proof-of-concept for simple and safe point-source oxidation of pharmaceutical compounds in fresh human urine.

2. Experimental Section

2.1 Chemicals and Solutions

Ultrapure water (>18.2 MΩ/cm resistance) was used for preparation of all standards and test solutions. Reagent grade (99% purity or higher) $(NH_2)_2CO$, NaCl, $NaHCO_3$, NH_4OH, NH_4Cl, HCl, $NaClO_3$, $NaClO_4$, $HgCl_2$, $Na_2S_2O_3$, Na_2SO_4, $NaNO_3$, $NaNO_2$, glycine, creatinine, uric acid, and urea obtained from Sigma-Aldrich were used for all standards and test solutions. DPD free and total chlorine test kits were obtained from Sigma-Aldrich. NaOCl (Sigma-Aldrich; 13.5% available chlorine) stock solution was calibrated every month by iodometry. Catalase (Sigma-Aldrich) was vortexed and centrifuged to remove the supernatant, then reconstituted in phosphate buffer and centrifuged again, with the process repeated 5 times to remove thymol. Analytical reference standards of cyclophosphamide (CP) (90% purity) and sulfamethoxazole (SMX) (≥ 98% purity) from Sigma-Aldrich were used. Simplified synthetic fresh urine matrixes consisted of an aqueous solution of 250 mM urea, 100 mM NaCl, and either 1.92 mM CP or 0.39 mM SMX. Synthetic fresh urine matrix solutions consisted of 250 mM urea, 100 mM NaCl, 16 mM Na_2SO_4, 24 mM NaH_2PO_4, 13 mM creatinine, 3 mM uric acid, and 1.92 mM CP or 0.39 mM SMX. All prepared synthetic fresh urine matrixes were at pH 6. Synthetic hydrolyzed urine matrixes consisted of an aqueous solution of 250 mM $NaHCO_3$, 100 mM NH_4Cl, and 400 mM NH_4OH (i.e., $[NH_4^+]_{total}$ = 500 mM) at pH 9.35. Synthetic hydrolyzed aged urine matrixes were adapted from Udert et al.[35] and Hoffmann et al.[16], and consisted of 250 mM $NaHCO_3$, 100 mM NaCl, and either 140 mM or 33 mM NH_4OH at pH 9.02 and 8.88, respectively. Authentic fresh urine was collected at 10 A.M. and blended from 6 people, 3 males and 3 females, with different ethnic background and diets. The blended urine was pH 6.3. Electrolysis of authentic fresh urine was started immediately after the addition of 0.39 mM SMX to 40 mL of the blended urine.

2.2 Electrolytic Cell and Electrodes

A custom three-electrode electrochemical cell was used for all oxidation experiments in this work (**Figure S1**). Detailed schematic dimensions and a photograph of the cell are provided in the SI (**Figure S2).** The cell was designed to accommodate a large planar working electrode with dimensions 40 mm x 80 mm, which is held in place between the bottom of the cell and a base plate. A seal is formed with a Kalrez gasket exposing a planar surface area of the working electrode of 8.56 cm^2. Planar anodes (BDD or IrO_2) were used for the oxidation experiments. SAE 304 stainless steel tubes were used as the counter electrodes in all oxidation experiments. An Ag/AgCl (3 M NaCl) reference electrode (BASi, West Lafayette, IN, USA) was used in all experiments. In the "undivided cell" setup, the counter electrode was immersed in the same solution as the working electrode. In the "divided cell" setup, the counter electrode was placed inside a glass tube with a 12 mm O.D. porous frit at the bottom (4-8 μm pores, ACE Glass #7209 porosity E). For oxidation experiments, three counter electrodes in fritted glass tubes were used in parallel to minimize resistance and potential drop due to ionic transport through the frits.

Planar boron-doped diamond (BDD) electrodes were purchased from Condias GmbH. Planar Ti/IrO_2 electrodes were prepared by thermal decomposition of a 250 mM H_2IrCl_6 precursor solution similar to a method described previously.[35] Ti sheet metal was first sandblasted and cleaned with 1 M oxalic acid for 1 hour at 95 °C. The precursor solution was spray-coated onto the Ti substrates on a hotplate held at 500 °C, and then the substrates were annealed at 500 °C for 1 hr after precursor deposition.

2.3 Electrochemical Methods

All cyclic voltammetry, galvanostatic, and potentiostatic experiments were performed with a Princeton Applied Research Potentiostat/Galvanostat Model 263A.

Cyclic Voltammetry of Anode Reactions: Each electrode (BDD and IrO_2) was sonicated in deionized water then pretreated in 40 mL 100 mM Na_2SO_4 for 5 minutes at 3.5 V or 2 V respectively. The electrochemical cell was then thoroughly rinsed with deionized water. The matrix of interest was then added to the cell and a single scan was initiated from 0 V to 3.5 V or 2.5 V respectively, and back to 0 V at a scan rate of 50 mV/s in the undivided cell setup. Nitrogen gas was bubbled through the solution for two minutes prior to and blanketed during the cyclic voltammetry.

Galvanostatic Oxidation of Pharmaceuticals in Urine: Electrochemical oxidations of pharmaceutical compounds were performed galvanostatically at a current density of 10 mA/cm^2 for 120 min (reaching 4.2 A-h/L) while the solution was stirred at 550 rpm. These experiments were conducted in a supporting electrolyte with the major constituents of synthetic fresh urine (100 mM NaCl and 250 mM urea, pH 6.15) or full synthetic fresh urine matrixes (*see above*) or synthetic hydrolyzed, aged urine matrixes (i.e., [NH_4^+/NH_3] = 33 or 140 or 500 mM, [HCO_3^-/CO_3^{2-}] = 250 mM and pH 9) and SMX or CP at a concentration of 0.39 mM or 1.92 mM, respectively. Based upon the suggested dosage from U.S. FDA[64, 65] and percentage of excretion via urine,[66, 67] SMX and CP will remain in human urine at concentrations of 0.975 mM and 1.92 mM, respectively. While the solubility of SMX is 610 mg/L (2.41 mM) at 37 °C,[68] dissolving this concentration of SMX at room temperature was difficult. Therefore, 100 mg/L SMX (0.39 mM) was used for electrolysis at room temperature. Aliquots were periodically collected, quenched with excess thiosulfate, and analyzed for target compounds and oxidation byproducts.

Galvanostatic Oxidation of Urine without Pharmaceuticals: Electrochemical oxidations of various urine matrixes were performed galvanostatically at a current density of 93 mA/cm^2 on BDD electrode for 90 min (reaching 30 A-h/L), stirred at 550 rpm. These experiments were

conducted in the supporting electrolytes that simulated different urine matrixes (simplified vs full urine matrixes, fresh vs. hydrolyzed, ammonia loss vs. no ammonia loss). A control experiment was conducted in NaCl solution to yield maximal oxychloride generation as a reference.

2.4 Analytical Methods

Aliquots were taken during electrolysis for analyses by ion chromatography (IC) and high-pressure liquid chromatography with ultraviolet absorbance and mass spectrometry detection (HPLC-UV-MS) (**Text S2**). pH was measured by an Apera pH60 pH tester. Free chlorine (FC), total chlorine (TC) and ClO_2 were measured by DPD and/or ABTS methods when electrolysis was employed in various urine matrixes (**Text S3**).

3. Results and Discussion

3.1 Advantages of Decentralized Treatment of Urine

Point-source electrochemical oxidation of pharmaceuticals in source-separated urine has multiple advantages compared with centralized treatment at a WWTF after it mixes with feces and other wastewater (**Table 1)**. These advantages are: (1) small treatment volumes, (2) high pharmaceutical concentration, (3) absence of non-urine derived background organic carbon or other interfering matrix constituents, and (4) high electrical conductivity. Average human urine production is 1.3 L/(person·day), while average domestic wastewater discharge is two orders of magnitude higher at 148 L/(person·day).[69] The dilution of urine with other waste streams not only decreases the absolute concentration of pharmaceuticals, but also decreases their relative concentration compared to the total concentration of organics in the solution (due to mixing with feces, cooking oils, detergents, etc.). This domestic wastewater may be further diluted by other waste streams containing other organics (such as industrial wastewater, urban runoff, etc.) before

reaching a WWTF. The daily per capita load of chemical oxygen demand (COD) to domestic wastewater from all sources (e.g., including feces, urine, greywater, etc.) is more than 6x higher than from urine alone, and the COD_{pharm}/COD_{total} is correspondingly 3.8% for domestic wastewater compared to 24.2% for urine (**Table 1**). Furthermore, the typical conductivity of fresh urine is two orders-of-magnitude higher than domestic wastewater. The combination of large treatment volumes and low conductivity for domestic wastewater streams would correspond to massive ohmic losses in the solution, making electrochemical oxidation as a "polishing" or tertiary WWT step even more costly.

Table 1. Comparison of relative advantages of degrading pharmaceuticals in urine before dilution with other domestic wastewater. [69, 70]

Matrix	Wastewater Contribution [L/person/day][a]	Conductivity [mS/cm][a]	Daily Per Capita COD Load [mg O_2/ person/ day]	Matrix COD [mg/L]	Pharm COD [mg/L]	Pharm COD/ (Pharm COD +Matrix COD)	Required Charge Passed [A·hr][b]	Electricity Cost [$/person/ day][b]	Electricity Cost [$/person/ year][b]
Pharmaceuticals Only	--	--	2080	--	--	--	29.0	$0.022	$7.95
Urine (including pharmaceuticals)	1.3	160	15080	10000	1600	13.8%	210	$0.16	$57.60
Domestic Wastewater	148	1.8	106080	702.7	14.05	2.0%	1480	$1.11	$405

[a] Dilution with other wastewater increases the treatment volume and reduces the matrix conductivity by two orders of magnitude. Pharmaceuticals are at their highest absolute and relative concentration when they are in urine, before they are diluted by other domestic wastewater sources. [b] To estimate the electricity cost of electrochemically oxidizing all organics in the matrix, chemical oxygen demand (COD) was used. The assumptions for these calculations are an electricity cost of 0.15 $/kWhr, a pharmaceutical concentration of 10 mM, a COD of 5 mols O_2/mol pharmaceutical, a total applied voltage of 5 V, a Faradaic efficiency toward oxidant reaction with organics of 30%, and full mineralization of pharmaceuticals to CO_2, H_2O, etc.

3.2 Reactive Chlorine Species Scavenged by Urea

Cyclic voltammetry was performed in three different solutions to reveal the effects of urea on the electrocatalytic oxidation of water (primarily to O_2(g) and $^{\bullet}OH$) and chloride (primarily to Cl_2(g), HOCl, $Cl^{\bullet}$, and $Cl_2^{\bullet-}$) by boron-doped diamond (BDD) and thermally decomposed iridium

oxide (IrO_2) anodes. BDD was used as a model "non-active" electrode that only physisorbs $^{\bullet}OH$, whereas IrO_2 was used as a model "active" electrode that chemisorbs $^{\bullet}OH$, effectively forming a surface hydroxyl group. The three solutions chosen comprised: (1) 100 mM $NaClO_4$ to characterize the water oxidation without chloride oxidation, given that ClO_4^- will not be further oxidized; (2) 100 mM NaCl to observe the additional current from chloride oxidation; and (3) 100 mM NaCl plus 250 mM urea to observe any differences in chloride oxidation that occur with urea present. **Figure 1a, b** shows cyclic voltammograms (CV) of oxidative sweeps of these three solutions on BDD and IrO_2. The CV of BDD with $NaClO_4$ shows the expected large onset potential for O_2(g) evolution of 2.4 V vs SHE.[71] With Cl^- present, the current onset potential shifts down to 2.1 V vs SHE due to the lower overpotential for Cl_2(g) evolution. See **Table S1** for a list of relevant thermodynamic standard and formal potentials for these reactions. In contrast to BDD, the CV of IrO_2 in **Figure 1b** showed a difference in the current onset potential and the magnitude of current when Cl^- is present. The IrO_2 surface oxidizes according to $IrO_2 + H_2O \rightleftharpoons IrO_3 + 2H^+ + 2e^-$.[72] In the Cl^- only solution on IrO_2, the peak seen in the cathodic sweep from 1.2 V to 0 V likely corresponds to the reduction of oxidized chlorine species such as HOCl, $Cl^{\bullet}$, or Ir-O-Cl surface groups. Most importantly, the absence of this peak when urea is present in the matrix shows that urea scavenges one or more of these reactive chlorine species (RCS).

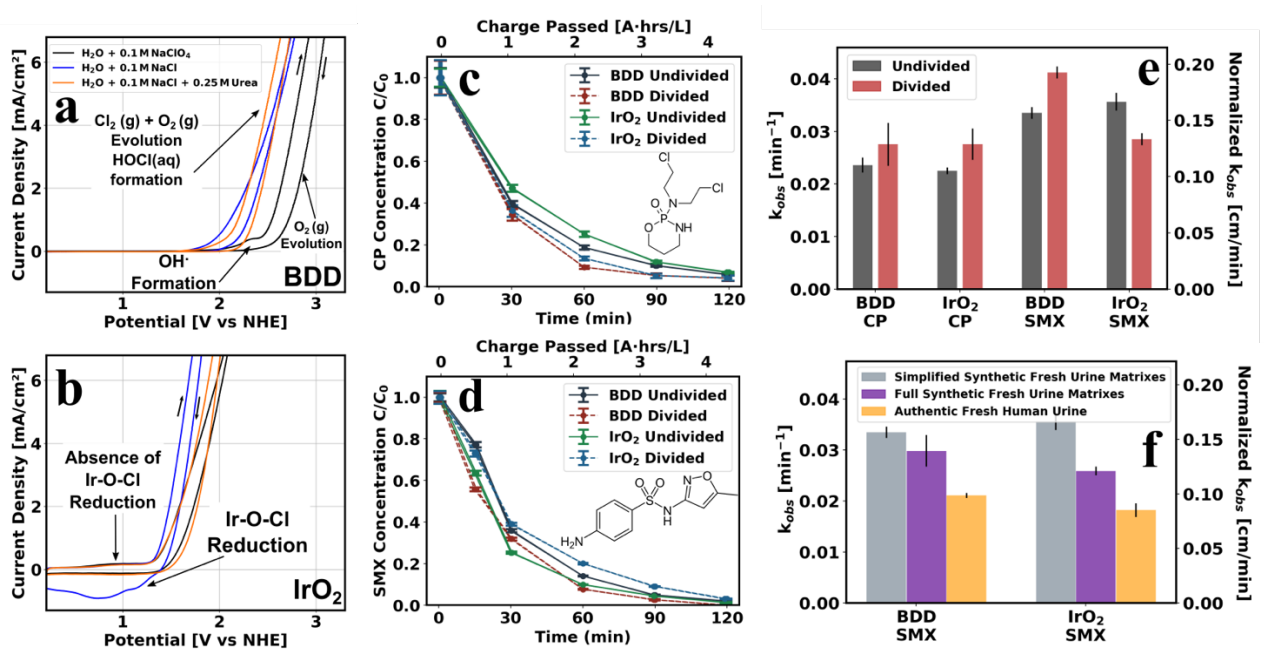

Figure 1. CVs in 100 mM $NaClO_4$, 100 mM NaCl, and 100 mM NaCl + 250 mM urea on (a) BDD and (b) IrO_2 anodes. On BDD, a lower onset potential of gas evolution when NaCl is present is indicative of $Cl_2(g)$ generation. On IrO_2 there are a couple of reduction peaks attributable to chlorine species (HOCl, $Cl^{\bullet}$ or Ir-O-Cl surface groups), apparent in the 100 mM NaCl matrix but absent in the $NaClO_4$ case. Interestingly, the reduction peaks are also absent when urea is added. This suggests that generated chlorine species are scavenged by urea. (c) Concentration of cyclophosphamide (CP) during the electrolysis in simplified synthetic fresh urine matrixes with a starting CP concentration of 1.9 mM. Inset: The chemical structure of CP. (d) Concentration of sulfamethoxazole (SMX) during oxidation in simplified synthetic fresh urine matrixes with a starting SMX concentration of 0.39 mM. Inset: The chemical structure of SMX. (e) Observed pseudo-first-order rate constants for pharmaceutical degradation. Note that the degradation rates in all conditions are fast enough to lower the concentration of pharmaceuticals by three orders of magnitude in five hours or less. (f) Observed pseudo-first-order rate constants for SMX degradation in simplified synthetic fresh urine, full synthetic fresh urine, and authentic fresh human urine with undivided electrochemical cell setup. The error bars represent standard deviations about the means from triplicate experiments.

3.3 Pseudo-First Order Kinetics and Mass Transfer

Most research thus far examining electrochemical oxidation of pharmaceuticals has reported rates of pharmaceutical degradation in terms of observed pseudo-first-order rate constants. As highlighted by Zöllig et al., these first-order kinetics should only be expected in galvanostatic

electrolysis for mass-transfer-limited reactions (assuming only heterogeneous reactions).[34] Therefore, the pseudo-first-order rate constants for pharmaceutical degradation are highly dependent on the geometry and the mass transport in the electrochemical setup. A mass-transfer limited observed pseudo-first-order rate constant is directly proportional to the planar surface-area of the anode and inversely proportional to the volume of the solution. In this work, an effort was made to choose reasonable values for the ratio of the electrode surface area to electrolyte volume (A/V) based on scale-up to a practical device. The electrochemical setup used in this work (**Figure S1)** has an A/V of 0.21 cm^{-1} and is magnetically stirred. The hydrodynamic flow pattern in the magnetically stirred reactor is similar[73] to the flow pattern in a rotating disk electrode (RDE),[74] where the mass-transfer limited reaction rate is proportional to $Re^{1/2}$ (Reynolds number, $Re = \omega r^2/\nu$). In order to assess if the electrochemical oxidation of pharmaceuticals is mass-transfer limited in our stirred electrochemical setup, we conducted galvanostatic oxidation experiments over a wide range of Reynolds number, $150 < Re < 10{,}000$. We found that the observed first-order rate constant for CP degradation varied linearly with $Re^{1/2}$ (**Figure S3**). This confirms that the experiments here are mass-transfer limited for CP. All experiments were performed with stir-bar radius (r) and rotation rates (ω) corresponding to $Re = 1{,}600$. This yields a mass-transfer limited electrolysis rate of 0.022 min^{-1} (i.e., 0.102 cm/min) for CP.

To determine what pseudo-first-order rate constants are practical for a real device, we modeled expected degradation rates for various rate constants as shown in **Figure S4**. A pseudo-first order rate constant of 0.01 min^{-1} or greater is required to lower pharmaceutical concentrations by at least three orders of magnitude in a 12-hour period, which is a reasonable residence time for a practical at-home situation. This corresponds to a geometry-normalized pseudo-first order rate constant

(based on A/V) of at least 0.05 cm/min to degrade pharmaceuticals at a rate reasonable for a scaled-up device.

3.4 Electrolysis of Pharmaceuticals

Galvanostatic oxidation in fresh-urine matrixes: A series of galvanostatic oxidations were performed with BDD and IrO_2 anodes. The experiments were performed on both anodes for two pharmaceuticals, SMX and CP (see chemical structures in **Figure 1c, d** insets). SMX and CP were chosen as test compounds because of their large differences in reactivity toward free chlorine (FC). SMX has a relatively high bimolecular rate constant with FC of ~10^3 $M^{-1}s^{-1}$ at circumneutral pH,[75] while we measured CP to be essentially non-reactive with FC (see **Text S4** for experimental details) (**Scheme 1**, r_{15}). Galvanostatic oxidations were performed in both an undivided electrochemical cell (working electrode (WE) and counter electrode (CE) in same compartment) and divided electrochemical cell (WE and CE separated by a frit) to test if cathodic reactions had any influence on the degradation pathway (see **Figure S1a** and **S1b**). The concentrations of SMX and CP were lowered by two orders-of-magnitude after two hours of electrolysis at 10 mA/cm^2 for all conditions (**Figure 1c** and **1d**). This corresponds to geometry normalized pseudo-first order rate constants greater than 0.1 cm/min for all conditions as shown in **Figure 1e**. As shown in **Figure 1f**, observed pseudo-first order rate constants of SMX degradation were lower for synthetic fresh urine matrixes and authentic fresh urine. However, the reactions remained sufficiently fast to degrade SMX by four orders of magnitude in ~8 hours as illustrated in **Figure S4**.

The rate constants for oxidation of both pharmaceuticals by both electrodes are similar in simplified synthetic fresh urine matrixes (i.e., urea + Cl^-). This suggests that mass transfer to the electrode surface is the dominant factor limiting the degradation rates (*see above*). For *Re = 10,000*, pseudo-first-order degradation rate constants up to 0.25 cm/min were achieved. However,

stir speeds corresponding to a *Re* number of 1,600 were used for the experimental data shown in **Figure 1**, since they are easy to achieve in electrochemical devices.

For the divided cell setup, a pH gradient is established because the oxygen evolution reaction (OER) at the anode generates H^+ while the hydrogen evolution reaction (HER) at the cathode generates OH^-. On average, the pH was stabilized to 1.8 for IrO_2 and 2.3 for BDD in the anode chamber and 12.5 in the cathode chamber for both electrodes. Furthermore, this gradient is quickly established. Passing 10 mA/cm^2 for 5 mins (~0.2 A·hr/L) was sufficient to establish this gradient of ~10 pH units for both BDD and IrO_2. Moreover, the electrolysis rates of CP and SMX did not show significant differences in divided and undivided cell setups. This suggests that there is little to no effect of cathodic reactions (possibly reducing homogeneous oxidants) on the degradation of pharmaceuticals, which is consistent with the above finding of mass-transfer limited degradation kinetics at the anode. In addition, the effect of the bulk solution pH (a drop from 6 in the undivided cell to 2 in the divided cell) had no appreciable impact on degradation rates. This could be due to the fact that the local pH at the anode surface in the undivided cell may be much lower than the bulk pH due to H^+ generation at the anode.

Differences between Synthetic Fresh, Hydrolyzed, and Hydrolyzed-Aged Urine Matrixes: The electrolysis rates of CP and SMX were also investigated in synthetic hydrolyzed and synthetic hydrolyzed aged urine matrixes and compared to a reference mass-transfer limited rate (**Figure 2a**). Sketches of concentration profiles adjacent to the anode surface are shown in **Figure 2b** to illustrate the differences between kinetic limitation (gradient A), mass-transport limitation due to heterogenous reactions (direct electron transfer and reactions with adsorbed $^{\bullet}OH$ or RCS) (gradient B), and mass-transport limitation due to the combination of heterogeneous reactions and near-anode-surface homogeneous reactions with desorbed $^{\bullet}OH$, RCS, or other homogeneous oxidants

(gradients C and D). As noted above, the mass-transfer limited electrolysis rate for CP was determined to be 0.022 min^{-1}. Given CP's slow reaction with RCS and the short lifetime of $^{\bullet}OH$, 0.022 min^{-1} likely corresponds to the mass-transport limited rate with primarily heterogeneous reactions. Desorbed $^{\bullet}OH$ may exist in solution, but the homogeneous reaction zone where it may react with CP is less than 1 μm in thickness,[76] which is small compared to the stagnant layer thickness of >20 μm. Additionally, the linear relationship between k_{obs} and $Re^{1/2}$ also suggests the obtained mass-transfer limiting rate corresponds to gradient B.

As shown in **Figure 2a**, the degradation rates of CP were mass-transfer limited in simplified and full synthetic fresh urine matrixes – likely due to the electro-generation of $^{\bullet}OH$ on the BDD anode. In comparison, the electrolysis rates of SMX exceeded the heterogeneous reaction mass-transfer limiting rate (gradient B). This suggests SMX degradation also occurs through homogeneous reactions involving either reactive chlorine species (RCS – a collective sum of FC and chlorine radicals) or other homogeneous oxidants (**Figure 2b**, Gradient C or D). In contrast, the electrolysis rates of CP and SMX were significantly decreased below the mass-transfer limiting rates in synthetic hydrolyzed urine matrixes amended with varying NH_4^+/NH_3 levels (to reflect different degrees of aging). This suggests that HCO_3^-/CO_3^{2-} (present at the same 250 mM concentration in each hydrolyzed urine matrix) acts as a dominant $^{\bullet}OH$ and $Cl^{\bullet}/Cl_2^{\bullet-}$ scavenger in such matrixes. This results in the formation of $CO_3^{\bullet-}$, which typically reacts with organic contaminants ~10^3-fold slower than $^{\bullet}OH$ or $Cl^{\bullet}$ and ~10-fold slower than $Cl_2^{\bullet-}$ (*see above*). Furthermore, the degradation rates of both pharmaceuticals in such matrixes were invariant with changes in the concentration of NH_4^+/NH_3, consistent with the apparent low reactivity of NH_4^+/NH_3 toward $CO_3^{\bullet-}$.[77] This likewise suggests that RCS do not contribute significantly to CP or SMX oxidation in the hydrolyzed urine matrixes, because increasing concentrations (33-500

mM) of NH_4^+/NH_3 would have been expected to increase RCS scavenging efficiency, and consequently decrease rates of pharmaceutical degradation if RCS were predominant oxidants. Furthermore, the electrolysis of CP and SMX appears to be kinetically limited in hydrolyzed urine matrixes (**Figure 2b**, Gradient A) for BDD anodes. As a result, it may be advantageous to electrochemically oxidize pharmaceuticals in fresh urine rather than in hydrolyzed urine for faster pharmaceutical removal.

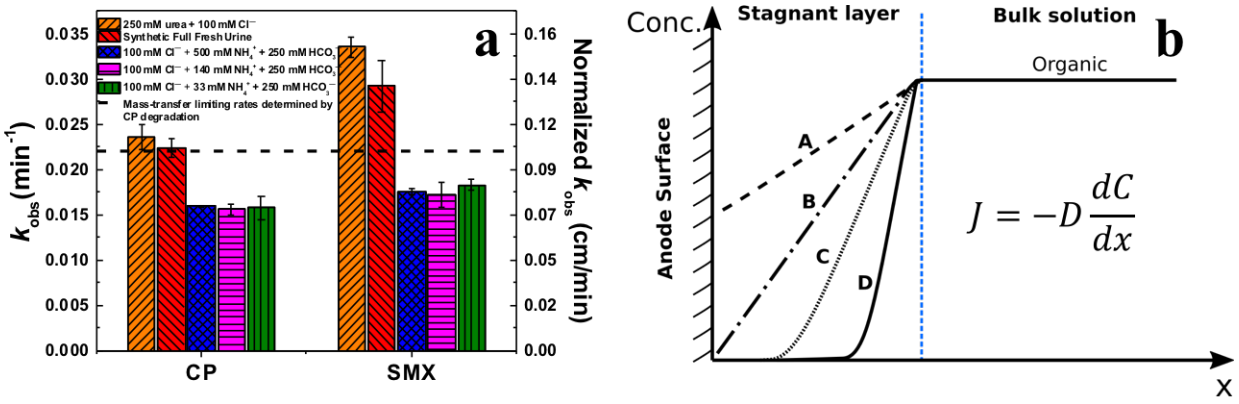

Figure 2. (a) Observed and geometry-normalized pseudo-first-order rate constants for pharmaceutical degradation on BDD electrodes with undivided cell setup in: (1) simplified urine matrixes (250 mM urea and 100 mM Cl^-, pH 6.15); (2) synthetic full fresh urine matrixes (see **Chemicals and Solutions,** pH 5.87); (3) hydrolyzed, un-aged urine matrixes (100 mM Cl^-, 500 mM NH_4^+ and 250 mM HCO_3^-, pH 9.35); (4) hydrolyzed, aged urine matrixes adapted from Udert et al.[35] (100 mM Cl^-, 140 mM NH_4^+ and 250 mM HCO_3^-, pH 9.02); and (5) hydrolyzed, aged urine matrixes adapted from Hoffmann et al. (100 mM Cl^-, 33 mM NH_4^+ and 250 mM HCO_3^-, pH 8.88). The dotted line represents the mass-transfer limiting rate of pharmaceutical degradation obtained from **Figure S3.** The electrolytes (40 mL) were stirred at 500 rpm. The applied current density was 10 mA/cm^2. The error bars represent standard deviations about the means from triplicate experiments. (b) Possible concentration gradients of pharmaceuticals in the stagnant layer (assuming constant bulk concentration). Gradient A: oxidation that is kinetically limited by the heterogenous reactions at the anode surface (i.e., via direct anodic oxidation and surface bound oxidants). Gradient B: the oxidation is mass-transfer limited and the concentration is zero at the anode surface, but increases in solution. Gradient C: the oxidation is mass-transfer limited, but in addition to heterogeneous reactions, oxidants generated at the anode desorb, diffuse outward, and react homogeneously with the pharmaceutical to drive the concentration to zero some distance away from the surface. Gradient D: the oxidation is mass-transfer limited with a larger homogeneous reaction enhancement than gradient C.

3.5 Generation of Oxidation Byproducts

The rates of oxidation byproduct generation in full synthetic fresh urine matrixes were compared for each combination of anode and cell configuration as shown in **Figure 3**. Both ClO_4^- and ClO_3^- were often found to be near or below the detection limits (i.e., 2 μM) for the ion chromatography techniques used in these experiments. The detection limits for both ClO_3^- and ClO_4^- were higher than in pure water due to the high concentration of Cl^- in urine matrixes. No ClO_4^- was measured in matrixes oxidized by the IrO_2 anode, which is similar to what has been reported previously.[16, 31] ClO_4^- was formed in the matrixes oxidized on the BDD anode, but at much lower concentrations than what has been reported previously.[16, 35] Additionally, the ClO_4^- measured on the BDD electrode was at a lower concentration than the ClO_3^-, which is consistent with other reports.[16, 35] Nitrate (NO_3^-) (**Figure 3c**) and nitrite (NO_2^-) (**Figure 3d**) generation were found to be higher on the IrO_2 electrode than the BDD electrode, though in IrO_2 divided cell experiments, NO_2^- generation was below the detection limit (5 μM). These oxidized nitrogen anions could come from the oxidation of urea, creatinine, uric acid and/or the oxidation of CP or SMX. Reaction pathways involving radical-driven generation of reactive nitrogen species from NO_3^- or NO_2^- have been shown to lead to potentially harmful nitrated and nitrosated byproducts.[78, 79] The suppression of NO_2^- formation when using the IrO_2 anode in the divided cell configuration indicates that such pathways would not be active or would at least be diminished and represents a potential advantage of operating in this mode.

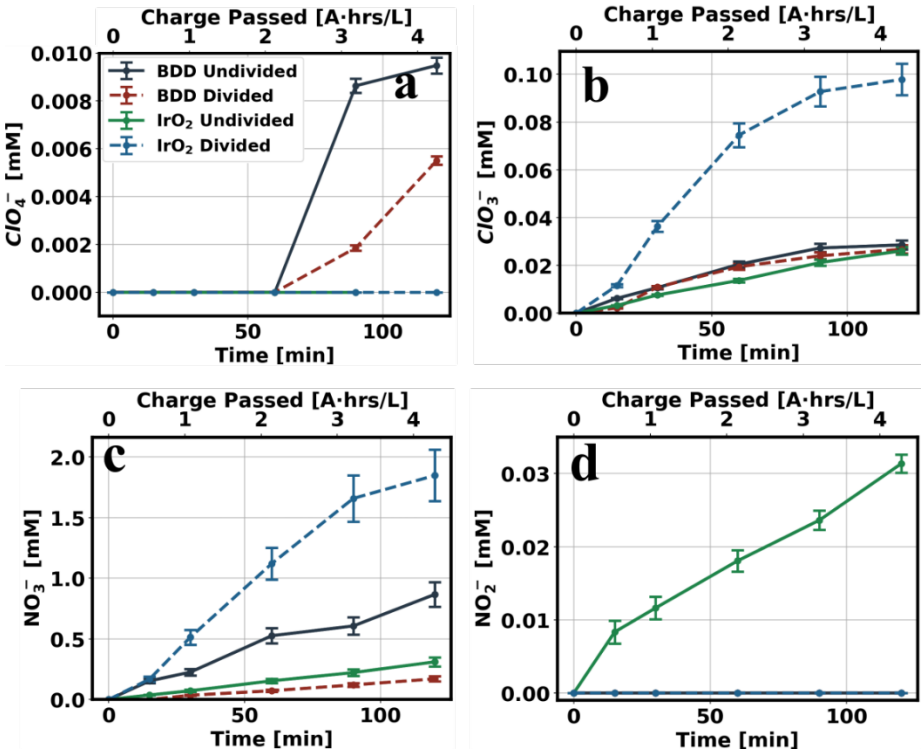

Figure 3. Evolution of inorganic oxidation byproducts showing concentrations of (a) ClO_4^-, (b) ClO_3^-, (c) NO_3^-, and (d) NO_2^- during electrolysis at 10 mA/cm^2 on BDD and IrO_2 anodes in the undivided and divided setups. Results are from oxidation of full synthetic fresh urine matrixes amended with 1.9 mM CP and 0.39 mM SMX. The error bars represent standard deviations from triplicate experiments. It is notable that the inorganic oxidation byproduct concentrations observed here in full synthetic fresh urine matrixes are substantially lower than what have been previously reported in authentic hydrolyzed aged urine.[16, 35]

Inhibition of Oxychloride Formation Increases with Increased Urea or NH_4^+/NH_3: The levels of generated OBPs shown in **Figure 3** are substantially lower than in previous studies of authentic hydrolyzed aged urine electrolysis.[16, 35] Therefore, further experiments were undertaken in several matrixes and at extended electrolysis time to evaluate potential causes of the lower rates of formation of OBPs (**Figure 4**). Fresh urine has an average concentration of 250 mM urea,[36] whereas hydrolyzed urine should exhibit maximal concentrations of 500 mM NH_4^+/NH_3 and 250 mM HCO_3^- after urea hydrolysis. Previous studies that have examined the treatment of authentic hydrolyzed aged urine have typically utilized much lower NH_4^+/NH_3 concentrations (e.g., 34 mM[16] and 109 mM[35]) indicating substantial ammonia loss during storage (aging). As shown in **Figure**

4, ClO_3^- and ClO_4^- generation were increasingly inhibited as dissolved nitrogen concentration increased. For example, a 10^3-fold decrease in ClO_3^- and ClO_4^- generation was observed for a matrix of 100 mM Cl^- and 250 mM urea compared to 100 mM Cl^- alone. A full synthetic fresh urine matrix containing the other primary constituents of urine (citrate, creatinine, uric acid, SO_4^{2-}, and $H_2PO_4^-$) also showed exceptionally low ClO_3^- and ClO_4^- generation. A matrix representing hydrolyzed (but not aged) urine (100 mM Cl^-, 500 mM NH_4^+, and 250mM HCO_3^-) yielded a roughly 10^2-fold lower ClO_3^- concentration than 100 mM Cl^- alone, whereas ClO_4^- levels generated were similar to those observed in the presence of 250 mM urea. The dashed lines in **Figure 4** indicate concentrations 100x higher than the suggested drinking water limits for each oxychloride species. Assuming that urine is typically diluted by a factor of greater than 100 in transit to WWTFs, these lines are intended to represent thresholds below which ClO_3^- and ClO_4^- levels would not exceed the WHO drinking water guidelines of 700 µg/L for ClO_3^- or 70 µg/L for ClO_4^- even for a "worst-case" scenario of minimal WWTF effluent dilution such as direct potable reuse.[80] As evident from **Figure 4**, ClO_3^- and ClO_4^- levels in all of the matrixes containing low or no NH_4^+/NH_3 exceeded these thresholds, whereas ClO_3^- and ClO_4^- levels in the high NH_4^+/NH_3 and urea-containing matrixes were below the thresholds (except for ClO_3^- in the high NH_4^+/NH_3 matrix at the highest values of charge passed).

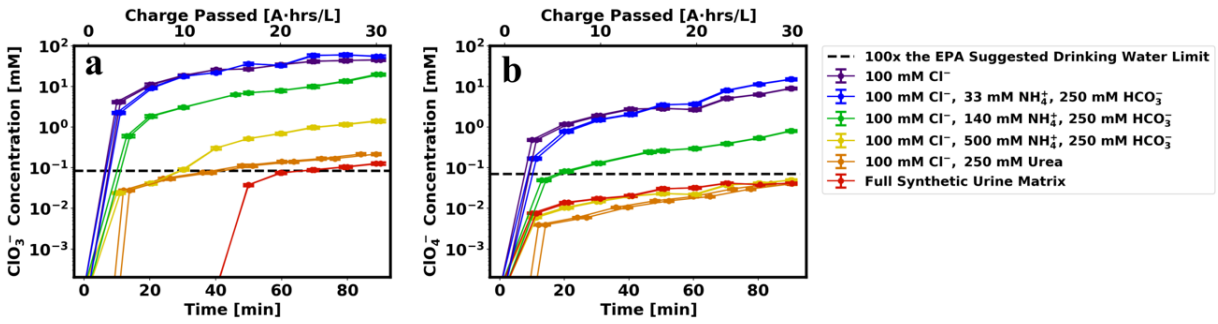

Figure 4. OBP formation in galvanostatic electrolysis experiments undertaken over extended times compared to experiments from which the Figure 3 data were obtained. Concentrations of generated (a) ClO_3^- and (b) ClO_4^- were measured for various matrixes treated using a BDD anode in the undivided setup. For the matrixes containing NH_4^+/NH_3, the pH was 9–10. For the matrixes containing only Cl^- and/or urea, the pH was 6–7. Galvanostatic treatments were performed for 90 mins at a current density of 93 mA/cm^2 for a final charge passed of 30 A·hr/L. The dashed lines indicate concentrations 100x higher than suggested drinking water limits for each oxychloride species (see accompanying discussion in the main text).

Mechanism of Inhibition of Oxychloride Formation: In a chloride solution, oxidation of Cl^- to $HOCl/OCl^-$ is expected to proceed through direct oxidation or reaction with $^{\bullet}OH$ at or near the electrode surface (**Scheme 1**, $r_{5\text{-}10}$).[15, 81] Subsequently, $HOCl/OCl^-$ is oxidized at or near the BDD electrode surface via direct electron transfer and/or reaction with $^{\bullet}OH_{ads}$ to form ClO_3^- and ClO_4^- (**Scheme 1**, $r_{16\text{-}18}$).[51, 82] In this study, we have shown that increasing urea or NH_4^+/NH_3 inhibits the formation of ClO_3^- and ClO_4^-. We hypothesize that high urea or NH_4^+/NH_3 concentrations effectively prevent oxychloride formation by: (1) scavenging chlorine radical species (**Scheme 1**, r_{11} and r_{12}) and/or (2) reacting with $HOCl/OCl^-$ and thereby sequestering chlorine in the form of organic chloramines (N-chlorinated urea) or inorganic chloramines (NH_2Cl, $NHCl_2$, and/or NCl_3) (**Scheme 1**, r_{13} and r_{14}). Either pathway would block key steps in the pathways of Cl^- oxidation to ClO_3^- and ClO_4^-.

Free chlorine (FC; comprising Cl_2O, HOCl, OCl^- and Cl_2), total chlorine (TC; comprising FC and chloramines), and chlorine dioxide (ClO_2) in bulk solution were quantified in full synthetic fresh urine and various synthetic hydrolyzed urine matrixes to explore the mechanism whereby ClO_3^- and ClO_4^- formation is inhibited (**Figure 5**). The key observations from these measurements are: (1) ClO_2 was not detected at measurable concentrations in any of the matrixes investigated, consistent with the hypothesized action of urea or NH_4^+/NH_3 on RCS involved in steps preceding formation of ClO_2 in the Cl^- to ClO_4^- oxidation sequence (e.g., $Cl^{\bullet}$, $Cl_2^{\bullet-}$, $ClO^{\bullet}$, or FC); (2) no FC was measurable in the bulk solution in any of the matrixes; (3) high μM to low mM levels of

chloramine species (measured as the difference in TC and FC values) were present in each matrix, confirming that FC (once formed) was consumed by urea or NH_4^+/NH_3 to form chloramine species; and importantly (4) lower concentrations of chloramines were generated in the presence of higher concentrations of NH_4^+/NH_3 or urea. This last observation indicates that FC generation (followed by chloramine formation) is faster at lower concentrations of NH_4^+/NH_3. This suggests that at higher NH_4^+/NH_3 concentrations, the reaction between $Cl^{\bullet}/Cl_2^{\bullet-}$ and NH_4^+/NH_3 to generate $NH_2^{\bullet}$ (**Scheme 1**, r_{12}) out-competes the reactions between $Cl^{\bullet}/Cl_2^{\bullet-}$, $^{\bullet}OH$, and H_2O to generate HOCl (**Scheme 1**, $r_{8\text{-}10}$). The generated $NH_2^{\bullet}$ is then scavenged by dissolved O_2,[41] $^{\bullet}OH$,[83] $CO_3^{\bullet-}$,[84] etc. without formation of chloramines. A satisfactory explanation must also reconcile the fact that the rates of generation of ClO_3^- and ClO_4^- were found to be similar in NaCl-only electrolyte (no urea, no ammonium, no bicarbonate, etc.) and in synthetic hydrolyzed urine with low NH_4^+/NH_3 concentration (33 mM NH_4^+, 250 mM $HClO_3^-$) (**Figure 4**), even though bulk-solution FC was effectively sequestered as chloramine in the latter matrix (**Figure 5b**).

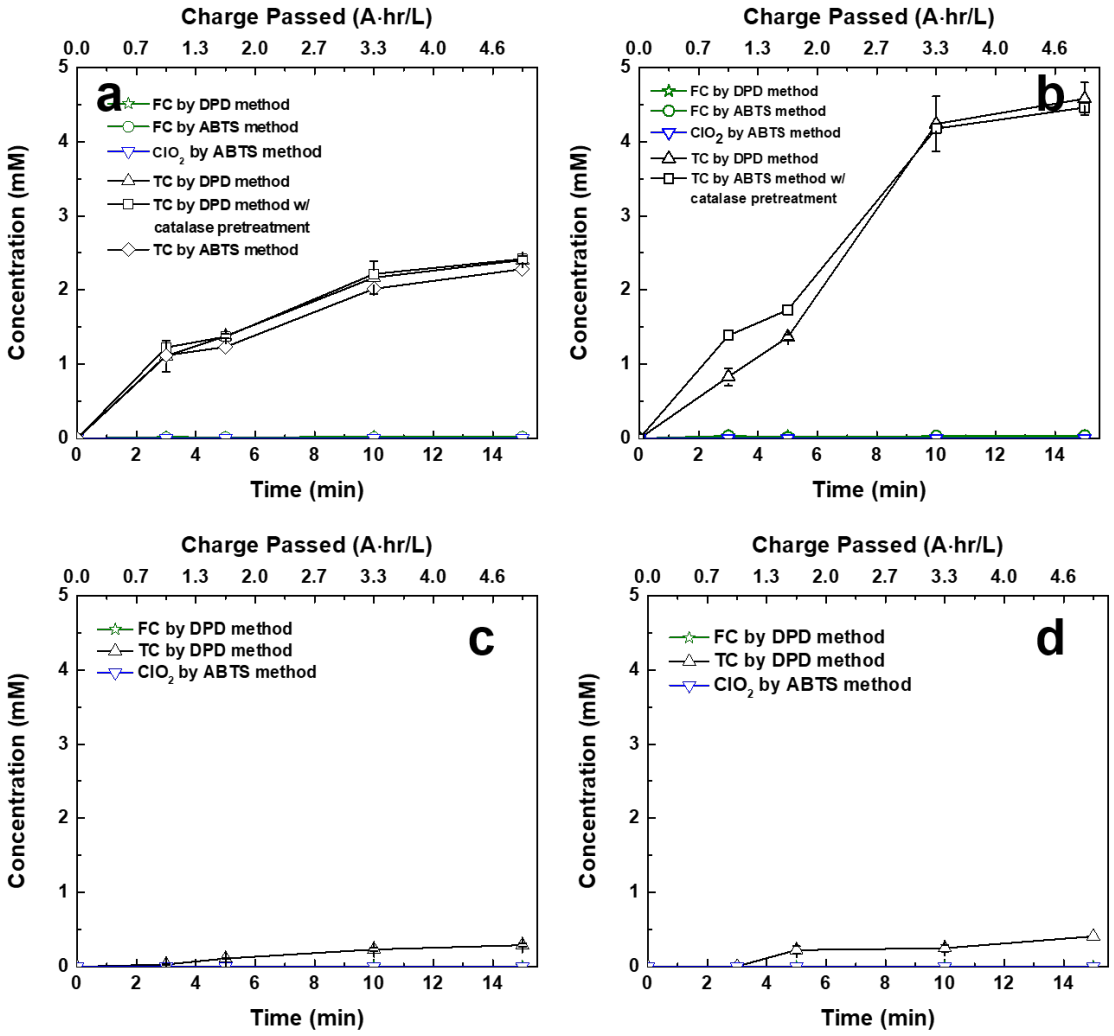

542

543 **Figure 5.** Concentration profiles of various chlorine species during electrolysis on the BDD anode in four
544 different matrixes. Starting from a baseline solution 100 mM Cl^-, 33 mM NH_4^+, 250 mM HCO_3^-, the four
545 solutions were: (a) baseline solution at pH 6.75. (b) baseline solution at pH 8.88; (c) baseline solution with
546 high ammonium (500 mM NH_4^+) at pH 9.35; (d) Full synthetic fresh urine matrix (no ammonium and
547 bicarbonate but with urea, creatine, uric acid, etc.) at pH 5.87). The current densities were 93.3 mA/cm^2;
548 the stir rate was 500 rpm. FC and ClO_2 were not measurable in any of the four matrixes investigated. FC
549 measurements via DPD were verified by ABTS in matrixes (a) and (b). The measurement of total chlorine
550 via DPD was checked by ABTS in matrix (a). Potential interference of H_2O_2 with the measurements of TC
551 was investigated by pretreating diluted samples with catalase to decompose any H_2O_2 that may have been
552 present. The absence of any effect from catalase treatment indicates that H_2O_2 was not present at
553 concentrations sufficient to interfere with TC measurements. Error bars represent standard deviation about
554 the means from triplicate experiments.
555

556 Taken together, these observations suggest that: (1) generation of ClO_3^- and ClO_4^- in these

557 systems involves oxidation of FC at or near the anode surface (as opposed to the bulk solution),

558 which is consistent with DFT calculations in previous work;[51, 82, 85] (2) lower levels of FC
559 formation for high urea and NH_4^+/NH_3 concentrations are linked to lower levels of ClO_3^- and ClO_4^-
560 formation; and (3) suppression of ClO_3^- and ClO_4^- formation by urea and NH_4^+/NH_3 derives from
561 their $Cl^\bullet$ and/or $Cl_2^{\bullet-}$ scavenging effects at or near the anode interface that precede formation of
562 HOCl/OCl^- (**Scheme 1**, $r_{11\text{-}12}$), rather than from FC scavenging effects in bulk solution or at the
563 interface (**Scheme 1**, r_{16}). Considering the much lower reactivity of urea than NH_4^+/NH_3 toward
564 $^\bullet OH$ (**Text S1**), scavenging of $^\bullet OH$ is unlikely to be the primary mechanism for the suppression of
565 oxychloride formation. This also points to scavenging of $Cl^\bullet$ or $Cl_2^{\bullet-}$ involved in FC formation as
566 a more likely explanation for the similar effects of urea and NH_4^+/NH_3 on ClO_4^- formation, and
567 the even somewhat greater effectiveness of urea in suppressing ClO_3^- formation. Finally, the fact
568 that similar amounts of ClO_3^- and ClO_4^- are formed in both NaCl-only and low NH_4^+/NH_3 (**Figure**
569 **4**) solutions suggests that NH_4^+/NH_3 becomes depleted near the anode surface at low
570 concentrations. This shuts-down the amino radical pathway (**Scheme 1**, $r_{11\text{-}12}$) leaving $Cl^\bullet$ or $Cl_2^{\bullet-}$
571 to form HOCl (**Scheme 1** $r_{6\text{-}10}$), which is then oxidized to form ClO_3^- and ClO_4^-.
572 The use of appropriately-selective probe compounds for quantification of $Cl^\bullet$, $Cl_2^{\bullet-}$, and/or $ClO^\bullet$
573 could provide more definitive evidence of the relative effects of urea and NH_4^+/NH_3 on chlorine
574 radical scavenging. Unfortunately, the probe compounds most commonly accepted for such uses
575 in advanced oxidation processes, such as nitrobenzene,[86-88] benzoic acid,[89] and 1,4-
576 dimethoxybenzene,[90, 91] are unsuitable for electrolysis in either divided or undivided cells due to
577 potential artifacts from their direct oxidation on anodes.[92-96] Overall, these results indicate that the
578 protective effect of ammonia in mitigating oxychloride formation during electrolysis of hydrolyzed
579 aged urine is likely to be lower than that afforded by urea in fresh urine due to ammonia losses
580 following urea hydrolysis.

4. Conclusion

This work demonstrates that urea (or NH_4^+/NH_3 from hydrolyzed urea) at the concentrations present in human urine can suppress the pathway(s) of Cl^- oxidation to the oxychlorides ClO_3^- and ClO_4^- during EAOPs. This fortuitous effect greatly inhibits the formation of the highly stable ClO_3^- and ClO_4^- ions, which are two of the most recalcitrant oxidation byproducts of EAOPs. The data show that pharmaceuticals could be degraded to less than 5% of their starting concentrations with less than 10 μM ClO_4^- and 100 μM ClO_3^- generated following 2 hours of electrolysis in matrixes containing 250 mM urea. These data demonstrate the feasibility of devices that eliminate pharmaceuticals in urine at the source of generation while generating minimal oxidation byproducts. "Non-active" BDD[15] has been the anode of choice for EAOPs because of high oxidizing power, but is prohibitively expensive to use in a practical device. This work demonstrates that "active" IrO_2[15] is sufficiently oxidizing to degrade cyclophosphamide (a particularly recalcitrant pharmaceutical) in simplified synthetic fresh urine matrixes at reasonably high rates of ~0.1 cm/min. Therefore, it highlights a large opportunity for the development of both "non-active" and "active" low-cost anodes that have long service lifetime. Device development based on this chemistry could provide an important contribution to mitigating the release of pharmaceuticals and other contaminants into the environment.

Associated Content

Supporting Information. Includes calculated $^{\bullet}OH$-scavenging rates in various matrixes, analytical methods for IC and HPLC-UV-MS, the procedure used to measure CP/HOCl reaction

kinetics, procedures for measurement of free and total chlorine, electrochemical cell schematics, results from mass transfer experiments, modeling of degradation rates for different pseudo-first-order rate constants, and tables of relevant electrochemical and chemical reactions.

AUTHOR INFORMATION

Corresponding Author

Email: h2@uw.edu

Author Contributions

These authors contributed equally: James A. Clark, Yuhang Yang. H.W.H. conceived the effort and supervised the execution of the research. J.A.C. designed the electrochemical cell, conceived of the experiments, and analyzed/plotted the data using custom python scripts. Y.Y. executed and designed experiments and analyzed the HPLC-UV-MS and IC data and developed python code. N.C.R. assisted in the execution of experiments and python code development. M.C.D. contributed knowledge and advice related to analytical methods and solution chemistry of free halogens, oxychlorides, and reactive oxygen and halogen species. All authors discussed the results and contributed to the final manuscript. All authors have given approval to the final version of the manuscript.

Funding Sources

We acknowledge primary financial support from the Rehnberg endowment.

Acknowledgment

We thank Prof. Ed Kolodziej (University of Washington-Tacoma and the UW Center for Urban Waters) for helpful scientific discussions. We also thank Prof. Ilwhan Oh (Kumoh National Institute of Technology, Korea) for useful discussions about cell design. We thank Dr. Martin Sadilek (University of Washington, Department of Chemistry) for training and helpful discussion on HPLC-UV-MS. We also thank J. Sean Yeung (University of Washington, Department of Civil and Environmental Engineering) for training and helpful discussion on IC. Additionally, we thank Jesse Yu (University of Washington, Department of Pharmaceutics) for helpful discussions about elimination routes for pharmaceuticals.

References

1. Luo, Y.; Guo, W.; Ngo, H. H.; Nghiem, D. L.; Hai, I. F.; Zhang, J.; Liang, S.; Wang, C. X., A review on the occurrence of micropollutants in the aquatic environment and their fate and removal during wastewater treatment. *The Science of the total environment* **2014,** *473-474*, 619-641.
2. Calero-Caceres, W.; Melgarejo, A.; Colomer-Lluch, M.; Stoll, C.; Lucena, F.; Jofre, J.; Muniesa, M., Sludge As a Potential Important Source of Antibiotic Resistance Genes in Both the Bacterial and Bacteriophage Fractions. *Environmental Science & Technology* **2014,** *48* (13), 7602-7611.
3. Gerrity, W. D.; Benotti, J. M.; Reckhow, A. D.; Snyder, A. S., Pharmaceuticals and Endocrine-Disrupting Compounds in Drinking Water. In *Biophysico-Chemical Processes of Anthropogenic Organic Compounds in Environmental Systems: Xing/Anthropogenic Organic Compounds*, John Wiley & Sons, Inc.: 2011; pp 233-249.
4. Chong, M. N.; Jin, B.; Chow, C. W. K.; Saint, C., Recent developments in photocatalytic water treatment technology: A review. *Water Research* **2010,** *44* (10), 2997-3027.
5. Moreira, C. F.; Boaventura, A. R. R.; Brillas, E.; Vilar, J. P. V. t., Electrochemical advanced oxidation processes: A review on their application to synthetic and real wastewaters. *Applied Catalysis B: Environmental* **2017,** *202*.
6. Panizza, M.; Cerisola, G., Direct and mediated anodic oxidation of organic pollutants. *Chemical Reviews* **2009,** *109* (12), 6541-6569.
7. Barazesh, J. M.; Prasse, C.; Sedlak, D. L., Electrochemical transformation of trace organic contaminants in the presence of halide and carbonate ions. *Environmental science & technology* **2016,** *50* (18), 10143-10152.
8. Ciriaco, L.; Anjo, C.; Pacheco, M. J.; Lopes, A.; Correia, J., Electrochemical degradation of Ibuprofen on Ti/Pt/PbO2 and Si/BDD electrodes. *Electrochimica Acta* **2009,** *54* (5), 1464-1472.

9. Domínguez, J. R.; González, T.; Palo, P.; Sánchez-Martín, J.; Rodrigo, M.; Sáez, C., Electrochemical degradation of a real pharmaceutical effluent. *Water, Air, & Soil Pollution* **2012,** *223* (5), 2685-2694.
10. Sopaj, F.; Rodrigo, A. M.; Oturan, N.; Podvorica, I. F.; Pinson, J.; Oturan, A. M., Influence of the anode materials on the electrochemical oxidation efficiency. Application to oxidative degradation of the pharmaceutical amoxicillin. *Chemical Engineering Journal* **2015,** *262*.
11. von Gunten, U., Oxidation processes in water treatment: are we on track? *Environmental science & technology* **2018,** *52* (9), 5062-5075.
12. Miklos, D. B.; Remy, C.; Jekel, M.; Linden, K. G.; Drewes, J. E.; Hübner, U., Evaluation of advanced oxidation processes for water and wastewater treatment–a critical review. *Water Research* **2018,** *139*, 118-131.
13. Prasse, C.; Stalter, D.; Schulte-Oehlmann, U.; Oehlmann, J.; Ternes, T. A., Spoilt for choice: a critical review on the chemical and biological assessment of current wastewater treatment technologies. *Water research* **2015,** *87*, 237-270.
14. Wang, N. N.; Zheng, T.; Zhang, G. S.; Wang, P., A review on Fenton-like processes for organic wastewater treatment. *Journal of Environmental Chemical Engineering* **2016,** *4* (1), 762-787.
15. Radjenovic, J.; Sedlak, D. L., Challenges and opportunities for electrochemical processes as next-generation technologies for the treatment of contaminated water. *Environmental Science & Technology* **2015,** *49* (19), 11292-11302.
16. Jasper, J. T.; Yang, Y.; Hoffmann, M. R., Toxic Byproduct Formation during Electrochemical Treatment of Latrine Wastewater. *Environmental Science & Technology* **2017,** *51* (12), 7111-7119.
17. Lienert, J.; B□rki, T.; Escher, I. B., Reducing micropollutants with source control: substance flow analysis of 212 pharmaceuticals in faeces and urine. *Water science and technology: a journal of the International Association on Water Pollution Research* **2005,** *56* (5), 87-96.
18. Lienert, J.; Gudel, K.; Escher, B. I., Screening method for ecotoxicological hazard assessment of 42 pharmaceuticals considering human metabolism and excretory routes. *Environmental Science & Technology* **2007,** *41* (12), 4471-4478.
19. Shargel, L.; Andrew, B.; Wu-Pong, S., *Applied biopharmaceutics and pharmacokinetics*. Appleton & Lange Stamford: 1999.
20. Wienkers, L. C.; Heath, T. G., Predicting in vivo drug interactions from in vitro drug discovery data. *Nature reviews Drug discovery* **2005,** *4* (10), 825.
21. Daniel, W., Metabolism of psychotropic drugs: pharmacological and clinical relevance. *Polish journal of pharmacology* **1995,** *47* (5), 367-379.
22. Buxton, G. V.; Greenstock, C. L.; Helman, W. P.; Ross, A. B., Critical review of rate constants for reactions of hydrated electrons, hydrogen atoms and hydroxyl radicals (· OH/· O– in aqueous solution. *Journal of physical and chemical reference data* **1988,** *17* (2), 513-886.
23. Garcia-Ac, A.; Broséus, R.; Vincent, S.; Barbeau, B.; Prévost, M.; Sauvé, S., Oxidation kinetics of cyclophosphamide and methotrexate by ozone in drinking water. *Chemosphere* **2010,** *79* (11), 1056-1063.
24. Zhang, R. C.; Yang, Y. K.; Huang, C. H.; Li, N.; Liu, H.; Zhao, L.; Sun, P. Z., UV/H2O2 and UV/PDS Treatment of Trimethoprim and Sulfamethoxazole in Synthetic Human Urine: Transformation Products and Toxicity. *Environmental Science & Technology* **2016,** *50* (5), 2573-2583.

25. Cotillas, S.; Lacasa, E.; Sáez, C.; Canizares, P.; Rodrigo, M. A., Electrolytic and electro-irradiated technologies for the removal of chloramphenicol in synthetic urine with diamond anodes. *Water research* **2018,** *128*, 383-392.
26. Jojoa-Sierra, D. S.; Silva-Agredo, J.; Herrera-Calderon, E.; Torres-Palma, A. R., Elimination of the antibiotic norfloxacin in municipal wastewater, urine and seawater by electrochemical oxidation on IrO anodes. *The Science of the total environment* **2017,** *575*, 1228-1238.
27. Cho, K.; Hoffmann, M. R., Urea Degradation by Electrochemically Generated Reactive Chlorine Species: Products and Reaction Pathways. *Environmental Science & Technology* **2014,** *48* (19), 11504-11511.
28. Urbańczyk, E.; Sowa, M.; Simka, W., Urea removal from aqueous solutions—a review. *Journal of Applied Electrochemistry* **2016,** *46* (10), 1011-1029.
29. Cotillas, S.; Lacasa, E.; Herraiz, M.; Sáez, C.; Cañizares, P.; Rodrigo, M. A., The Role of the Anode Material in Selective Penicillin G Oxidation in Urine. *ChemElectroChem* **2019,** *6* (5), 1376-1384.
30. Cotillas, S.; Lacasa, E.; Sáez, C.; Cañizares, P.; Rodrigo, M. A., Removal of pharmaceuticals from the urine of polymedicated patients: A first approach. *Chemical Engineering Journal* **2018,** *331*, 606-614.
31. Li, H.; Yu, Q. N.; Yang, B.; Li, Z. J.; Lei, L. C., Electro-catalytic oxidation of artificial human urine by using BDD and IrO2 electrodes. *Journal of Electroanalytical Chemistry* **2015,** *738*, 14-19.
32. Jasper, J. T.; Shafaat, O. S.; Hoffmann, M. R., Electrochemical Transformation of Trace Organic Contaminants in Latrine Wastewater. *Environmental Science & Technology* **2016,** *50* (18), 10198-10208.
33. Yang, Y.; Shin, J.; Jasper, T. J.; Hoffmann, R. M., Multilayer Heterojunction Anodes for Saline Wastewater Treatment: Design Strategies and Reactive Species Generation Mechanisms. *Environmental science & technology* **2016,** *50* (16), 8780-8787.
34. Zollig, H.; Remmele, A.; Morgenroth, E.; Udert, K. M., Removal rates and energy demand of the electrochemical oxidation of ammonia and organic substances in real stored urine. *Environmental Science-Water Research & Technology* **2017,** *3* (3), 480-491.
35. Zollig, H.; Remmele, A.; Fritzsche, C.; Morgenroth, E.; Udert, K. M., Formation of chlorination byproducts and their emission pathways in chlorine mediated electro-oxidation of urine on active and nonactive type anodes. *Environmental Science & Technology* **2015,** *49* (18), 11062-11069.
36. Rose, C.; Parker, A.; Jefferson, B.; Cartmell, E., The characterization of feces and urine: a review of the literature to inform advanced treatment technology. *Critical reviews in environmental science and technology* **2015,** *45* (17), 1827-1879.
37. Udert, M. K.; Larsen, A. T.; Biebow, M.; Gujer, W., Urea hydrolysis and precipitation dynamics in a urine-collecting system. *Water research* **2003,** *37* (11), 2571-2582.
38. Udert, K. M.; Larsen, T. A.; Gujer, W., Biologically induced precipitation in urine-collecting systems. *Water Science and Technology: Water Supply* **2003,** *3* (3), 71-78.
39. Udert, K. M.; Larsen, T. A.; Gujer, W., Estimating the precipitation potential in urine-collecting systems. *Water Research* **2003,** *37* (11), 2667-2677.
40. Armstrong, D. A.; Huie, R. E.; Koppenol, W. H.; Lymar, S. V.; Merényi, G.; Neta, P.; Ruscic, B.; Stanbury, D. M.; Steenken, S.; Wardman, P., Standard electrode potentials involving

radicals in aqueous solution: inorganic radicals (IUPAC Technical Report). *Pure and Applied Chemistry* **2015,** *87* (11-12), 1139-1150.
41. Neta, P.; Maruthamuthu, P.; Carton, P.; Fessenden, R., Formation and reactivity of the amino radical. *The Journal of Physical Chemistry* **1978,** *82* (17), 1875-1878.
42. Neta, P.; Huie, R. E.; Ross, A. B., Rate constants for reactions of inorganic radicals in aqueous solution. *Journal of Physical and Chemical Reference Data* **1988,** *17* (3), 1027-1284.
43. Mazellier, P.; Leroy, É.; De Laat, J.; Legube, B., Transformation of carbendazim induced by the H 2 O 2/UV system in the presence of hydrogenocarbonate ions: involvement of the carbonate radical. *New journal of chemistry* **2002,** *26* (12), 1784-1790.
44. Clifton, C. L.; Huie, R. E., Rate constants for some hydrogen abstraction reactions of the carbonate radical. *International journal of chemical kinetics* **1993,** *25* (3), 199-203.
45. Canonica, S.; Kohn, T.; Mac, M.; Real, F. J.; Wirz, J.; von Gunten, U., Photosensitizer method to determine rate constants for the reaction of carbonate radical with organic compounds. *Environmental science & technology* **2005,** *39* (23), 9182-9188.
46. Lei, Y.; Cheng, S.; Luo, N.; Yang, X.; An, T., Rate Constants and Mechanisms of the Reactions of Cl• and Cl2•–with Trace Organic Contaminants. *Environmental science & technology* **2019,** *53* (19), 11170-11182.
47. Xiao, S.; Qu, J.; Zhao, X.; Liu, H.; Wan, D., Electrochemical process combined with UV light irradiation for synergistic degradation of ammonia in chloride-containing solutions. *Water research* **2009,** *43* (5), 1432-1440.
48. Ji, Y.; Bai, J.; Li, J.; Luo, T.; Qiao, L.; Zeng, Q.; Zhou, B., Highly selective transformation of ammonia nitrogen to N2 based on a novel solar-driven photoelectrocatalytic-chlorine radical reactions system. *Water research* **2017,** *125*, 512-519.
49. Shen, Z.; Li, J.; Zhang, Y.; Bai, J.; Tan, X.; Li, X.; Qiao, L.; Xu, Q.; Zhou, B., Highly efficient total nitrogen and simultaneous total organic carbon removal for urine based on the photoelectrochemical cycle reaction of chlorine and hydroxyl radicals. *Electrochimica Acta* **2019,** *297*, 1-9.
50. Long, L.; Bu, Y.; Chen, B.; Sadiq, R., Removal of urea from swimming pool water by UV/VUV: The roles of additives, mechanisms, influencing factors, and reaction products. *Water research* **2019,** *161*, 89-97.
51. Hubler, D.; Baygents, J. C.; Chaplin, B.; Farrell, J., Understanding chlorite and chlorate formation associated with hypochlorite generation at boron doped diamond film anodes. *Journal of The Electrochemical Society* **2014,** *161* (12), E182-E189.
52. Buxton, G. V.; Bydder, M.; Salmon, G. A., Reactivity of chlorine atoms in aqueous solution Part 1The equilibrium Cl MNsbd+ Cl-Cl 2. *Journal of the Chemical Society, Faraday Transactions* **1998,** *94* (5), 653-657.
53. Qiang, Z.; Adams, C. D., Determination of monochloramine formation rate constants with stopped-flow spectrophotometry. *Environmental science & technology* **2004,** *38* (5), 1435-1444.
54. Blatchley III, E. R.; Cheng, M., Reaction mechanism for chlorination of urea. *Environmental science & technology* **2010,** *44* (22), 8529-8534.
55. Scialdone, O.; Guarisco, C.; Galia, A.; Herbois, R., Electroreduction of aliphatic chlorides at silver cathodes in water. *Journal of Electroanalytical Chemistry* **2010,** *641* (1-2), 14-22.
56. Sonoyama, N.; Sakata, T., Electrochemical continuous decomposition of chloroform and other volatile chlorinated hydrocarbons in water using a column type metal impregnated carbon fiber electrode. *Environmental science & technology* **1999,** *33* (19), 3438-3442.

57. Ma, J.; Yan, M.; Kuznetsov, A. M.; Masliy, A. N.; Ji, G.; Korshin, G. V., Rotating ring-disk electrode and quantum-chemical study of the electrochemical reduction of monoiodoacetic acid and iodoform. *Environmental science & technology* **2015,** *49* (22), 13542-13549.
58. Su, X.; Bromberg, L.; Tan, K.-J.; Jamison, T. F.; Padhye, L. P.; Hatton, T. A., Electrochemically mediated reduction of Nitrosamines by Hemin-Functionalized Redox electrodes. *Environmental Science & Technology Letters* **2017,** *4* (4), 161-167.
59. Brown, G. M., The reduction of chlorate and perchlorate ions at an active titanium electrode. *Journal of electroanalytical chemistry and interfacial electrochemistry* **1986,** *198* (2), 319-330.
60. Wang, D.; Huang, C.; Chen, J.; Lin, H.; Shah, S., Reduction of perchlorate in dilute aqueous solutions over monometallic nano-catalysts: Exemplified by tin. *Separation and Purification Technology* **2007,** *58* (1).
61. Wang, D.; Shah, S. I.; Chen, J.; Huang, C., Catalytic reduction of perchlorate by H2 gas in dilute aqueous solutions. *Separation and Purification Technology* **2008,** *60* (1), 14-21.
62. Yang, Q.; Yao, F.; Zhong, Y.; Wang, D.; Chen, F.; Sun, J.; Hua, S.; Li, S.; Li, X.; Zeng, G., Catalytic and electrocatalytic reduction of perchlorate in water ? A review. *Chemical Engineering Journal* **2016,** *306*.
63. Haynes, W. M., *CRC handbook of chemistry and physics*. CRC press: 2014.
64. BACTRIM (sulfamethoxazole and trimethoprim) injection, for intravenous use. https://www.accessdata.fda.gov/drugsatfda_docs/label/2017/018374s025lbl.pdf.
65. FDA, U. S. CYCLOPHOSPHAMIDE injection, for intravenous use. https://www.accessdata.fda.gov/drugsatfda_docs/label/2013/012141s090,012142s112lbl.pdf.
66. FDA BACTRIM™ sulfamethoxazole and trimethoprim DS (double strength) tablets and tablets USP. https://www.accessdata.fda.gov/drugsatfda_docs/label/2010/017377s067lbl.pdf.
67. Joqueviel, C.; Martino, R.; Gilard, V.; Malet-Martino, M.; Canal, P.; Niemeyer, U., Urinary excretion of cyclophosphamide in humans, determined by phosphorus-31 nuclear magnetic resonance spectroscopy. *Drug metabolism and Disposition* **1998,** *26* (5), 418-428.
68. Yalkowsky, H.; Press, Y. H. C., Handbook of Aqueous Solubility Data. By Samuel. 2003.
69. Larsen, T. A.; Udert, K. M.; Lienert, J., *Source separation and decentralization for wastewater management*. Iwa Publishing: 2013.
70. Putnam, D. F., Composition and concentrative properties of human urine. **1971**.
71. Kapałka, A.; Baltruschat, H.; Comninellis, C., Electrochemical Oxidation of Organic Compounds Induced by Electro - Generated Free Hydroxyl Radicals on BDD Electrodes. *Synthetic Diamond Films: Preparation, Electrochemistry, Characterization, and Applications* **2011**, 237-260.
72. Comninellis, C., Electrocatalysis in the electrochemical conversion/combustion of organic pollutants for waste water treatment. *Electrochimica Acta* **1994,** *39* (11-12), 1857-1862.
73. Halász, G.; Gyüre, B.; Jánosi, I. M.; Szabó, K. G.; Tél, T., Vortex flow generated by a magnetic stirrer. *American Journal of Physics* **2007,** *75* (12), 1092-1098.
74. Prentice, G., *Electrochemical engineering principles*. Prentice Hall: 1991.
75. Dodd, M. C.; Huang, C.-H., Transformation of the antibacterial agent sulfamethoxazole in reactions with chlorine: kinetics, mechanisms, and pathways. *Environmental science & technology* **2004,** *38* (21), 5607-5615.
76. Donaghue, A.; Chaplin, B. P., Effect of select organic compounds on perchlorate formation at boron-doped diamond film anodes. *Environmental science & technology* **2013,** *47* (21), 12391-12399.

77. Clarke, K.; Edge, R.; Johnson, V.; Land, E.; Navaratnam, S.; Truscott, T., The carbonate radical: its reactivity with oxygen, ammonia, amino acids, and melanins. *The Journal of Physical Chemistry A* **2008,** *112* (41), 10147-10151.
78. Hora, P. I.; Novak, P. J.; Arnold, W. A., Photodegradation of pharmaceutical compounds in partially nitritated wastewater during UV irradiation. *Environmental Science: Water Research & Technology* **2019,** *5* (5), 897-909.
79. Scholes, R. C.; Prasse, C.; Sedlak, D. L., The Role of Reactive Nitrogen Species in Sensitized Photolysis of Wastewater-Derived Trace Organic Contaminants. *Environmental science & technology* **2019**.
80. Organization, W. H., Guidelines for Drinking-Water Quality: Incorporating the First Addendum. Geneva, Switzerland. *World Health Organization* **2017**.
81. Jung, Y. J.; Baek, K. W.; Oh, B. S.; Kang, J.-W., An investigation of the formation of chlorate and perchlorate during electrolysis using Pt/Ti electrodes: The effects of pH and reactive oxygen species and the results of kinetic studies. *Water research* **2010,** *44* (18), 5345-5355.
82. Azizi, O.; Hubler, D.; Schrader, G.; Farrell, J.; Chaplin, B. P., Mechanism of perchlorate formation on boron-doped diamond film anodes. *Environmental science & technology* **2011,** *45* (24), 10582-10590.
83. Pagsberg, P. B., Investigation of the NH2 radical produced by pulse radiolysis of ammonia in aqueous solution. *Aspects of Research at Risø* **1972,** *5*, 209.
84. Draganić, Z. D.; Negron-Mendoza, A.; Sehested, K.; Vujošević, S. I.; Navarro-Gonzales, R.; Albarran-Sanchez, M.; Draganić, I. G., Radiolysis of aqueous solutions of ammonium bicarbonate over a large dose range. *International Journal of Radiation Applications and Instrumentation. Part C. Radiation Physics and Chemistry* **1991,** *38* (3), 317-321.
85. Chaplin, B. P., Critical review of electrochemical advanced oxidation processes for water treatment applications. *Environmental Science: Processes & Impacts* **2014,** *16* (6), 1182-1203.
86. Watts, M. J.; Linden, K. G., Chlorine photolysis and subsequent OH radical production during UV treatment of chlorinated water. *Water Research* **2007,** *41* (13), 2871-2878.
87. Nowell, L. H.; Hoigné, J., Photolysis of aqueous chlorine at sunlight and ultraviolet wavelengths—II. Hydroxyl radical production. *Water Research* **1992,** *26* (5), 599-605.
88. Fang, J.; Fu, Y.; Shang, C., The roles of reactive species in micropollutant degradation in the UV/free chlorine system. *Environmental science & technology* **2014,** *48* (3), 1859-1868.
89. Remucal, C.; Manley, D., Emerging investigators series: the efficacy of chlorine photolysis as an advanced oxidation process for drinking water treatment. *Environmental Science: Water Research & Technology* **2016,** *2* (4), 565-579.
90. Alfassi, Z.; Mosseri, S.; Neta, P., Reactivities of chlorine atoms and peroxyl radicals formed in the radiolysis of dichloromethane. *The Journal of Physical Chemistry* **1989,** *93* (4), 1380-1385.
91. O'Neill, P.; Steenken, S.; Schulte-Frohlinde, D., Formation of radical cations of methoxylated benzenes by reaction with OH radicals, Ti 2+, Ag 2+, and SO 4.-in aqueous solution. An optical and conductometric pulse radiolysis and in situ radiolysis electron spin resonance study. *Journal of Physical Chemistry* **1975,** *79* (25), 2773-2779.
92. Hess, E. Boron-doped Diamond Sensors for the Determination of Organic Compounds in Aqueous Media. University of the Western Cape, 2010.
93. Montilla, F.; Michaud, P.; Morallon, E.; Vazquez, J.; Comninellis, C., Electrochemical oxidation of benzoic acid at boron-doped diamond electrodes. *Electrochimica Acta* **2002,** *47* (21), 3509-3513.

882 94. Weinberg, N.; Marr, D.; Wu, C., Sensitive probe for double layer structure. Potential
883 dependent competitive cyanation and methoxylation of 1, 4-dimethoxybenzene. *Journal of the*
884 *American Chemical Society* **1975,** *97* (6), 1499-1504.
885 95. de Martinez, M. C.; Marquez, O.; Marquez, J.; Hahn, F.; Beden, B.; Crouigneau, P.;
886 Rakotondrainibe, A.; Lamy, C., In situ spectroscopic investigation of the anodic oxidation of 1, 4-
887 dimethoxybenzene at platinum electrodes. *Synthetic metals* **1997,** *88* (3), 187-196.
888 96. Jing, Y.; Chaplin, B. P., Mechanistic study of the validity of using hydroxyl radical probes
889 to characterize electrochemical advanced oxidation processes. *Environmental science &*
890 *technology* **2017,** *51* (4), 2355-2365.

891